Purdue University

Purdue e-Pubs

International Refrigeration and Air Conditioning Conference

School of Mechanical Engineering

2022

Thermodynamic Analysis of a Transcritical CO2 Heat Pump Integrating a Vortex Tube

Ahmed Mansour

Sébastien Poncet

Hakim Nesreddine

Follow this and additional works at: https://docs.lib.purdue.edu/iracc

Mansour, Ahmed; Poncet, Sébastien; and Nesreddine, Hakim, "Thermodynamic Analysis of a Transcritical CO2 Heat Pump Integrating a Vortex Tube" (2022). *International Refrigeration and Air Conditioning Conference.* Paper 2350.
https://docs.lib.purdue.edu/iracc/2350

This document has been made available through Purdue e-Pubs, a service of the Purdue University Libraries. Please contact epubs@purdue.edu for additional information.
Complete proceedings may be acquired in print and on CD-ROM directly from the Ray W. Herrick Laboratories at https://engineering.purdue.edu/Herrick/Events/orderlit.html

Thermodynamic Analysis of a Transcritical CO_2 Heat Pump Integrating a Vortex Tube

Ahmed MANSOUR[1*], Sébastien PONCET[1], Hakim NESREDDINE[2]

[1] Mechanical Engineering Department, Université de Sherbrooke, 2500 boulevard de l'Université, Sherbrooke (QC), J1K 2R1, Canada
ahmed.mansour@usherbrooke.ca, sebastien.poncet@usherbrooke.ca

[2] Laboratoire des Technologies de l'Énergie, Hydro-Québec, 600 Rue de la montagne, Shawinigan (QC), G9N 7N5, Canada
nesreddine.hakim@hydroquebec.com

* Corresponding Author

ABSTRACT

A thermodynamic model is implemented to study the performance of a transcritical CO_2 heat pump system integrating vortex tube. The study objective is to precisely prove that integrating a vortex tube is beneficial in raising the heat pump efficiency. The vortex tube is implemented to compensate the thermodynamic losses of the conventional expansion device and to produce more heated flow to raise the overall heating capacity of the heat pump. A validated thermodynamic model of the vortex tube was previously developed to operate with real gases and two-phase fluids and is implemented in the current study. However, for all other heat pump components, a commercial library TIL associated with the Dymola software is used to simulate the system. In addition, carbon dioxide is used as a working fluid due to its very minimal negative environmental effects, intoxicity and non-flammability and is operated under transcritical conditions. First of all, a conventional heat pump model (CHP) is validated to determine the feasibility of using the TIL library. Secondly, the vortex tube heat pump (VTHP) is compared to a CHP in terms of heating capacity and coefficient of performance (COP_h). The results show that VTHP can improve the heating capacity by 30.9% while COP_h can be refined by 31%. Finally, the VTHP system is analyzed parametrically to test the heat pump performance under different operating conditions: compressor discharge pressure (86-114 bar), desuperheater pressure (38-43 bar) and vortex tube cold mass fraction (0.2-0.8).

1. INTRODUCTION

Improving a heat pump system on different aspects has been carried out intensively throughout the past decades. These aspects can vary from building a complex system to just changing the refrigerant or one of the components. The purposes of such improvements are usually to increase the system efficiency, reduce losses and power consumption and make it more environmentally friendly.

In recent decades, many studies focused on testing different refrigerants that can be suitable for replacing the ones considered harmful to the environment. R22 was the most commonly used refrigerant in heat pumps (Chua *et al.*, 2010). However, even though it has an ozone depletion potential (ODP) of 0.05, deadlines were set to phase it out and to not produce it anymore due to the concerns of its impact on the ozone layer (Chen, 2008). R410a became the common substitution in heat pumps after the R22 due to its zero ozone depletion potential (Hakkaki-Fard *et al.*, 2015). However, its global warming potential (GWP) of 2088 is very high, even when compared to R22. Hence, better substitutions are needed to be found that provide at least the same operational performance with effects that are deemed acceptable on the environment.

Recently the focus has been shifted into using carbon dioxide (CO_2) as either single pure refrigerant or in a mixture with another refrigerant. CO_2 is a natural, non-toxic and non-flammable refrigerant that has a zero ODP and GWP of 1. Junqi *et al.* (2021) made a comparative study between CO_2 and R134a in heat pumps implemented in electric vehicles. They showed that at temperatures below -10 C^o, the heating capacity of the CO_2 system grew by 83% compared to the R134a system, even though the COP_h was 20-30 % lower. However, fixing the heating capacity at 4 kW for both systems, the COP_h of the CO_2 heat pump exhibited a 51 % advantage over the R134a system. Wang *et al.* (2018) also

conducted a study on a CO_2 heat pump that can be used in electric vehicles operating in cold weathers. They studied two heat pump configurations: a conventional heat pump configuration (CHP) and a secondary loop configuration (the secondary loop is inserted in place of the gas cooler after the compressor). The conventional cycle provided a COP_h of 3.1 and a heating capacity of 3.6 kW. However, the secondary loop cycle showed a reduction in COP_h by 19% and heating capacity by 6%. Moreover, the power consumed by the compressor increased by 15%.

Other researchers tried to overcome the operating disadvantage of CO_2 which is its low critical temperature by mixing it with another refrigerant. Hakkaki-Fard *et al.* (2015) compared the operation of a residential house heat pump using a mixture of R32 and CO_2 with variable proportions against R410a. They used R32 to eliminate the effect of low critical temperature of CO_2 while implemented CO_2 to create a non-flammable mixture. In terms of COP_h, an R32/CO_2 mixture of 90/10 proportionality exhibited the best performance followed by R410a. However, as CO_2 proportion increased, the heating capacity of the heat pump increased consequently with R410a showing the least performance. In addition, using a variable proportionality can save up to 23% of the seasonal energy consumption.

Improvements to heat pump systems have been developed through out history to enhance the efficiency and reduce excessive losses. Losses imposed by conventional throttling devices are one of the main sources of losses in heat pumps. Using a vortex tube can overcome this limitation. A vortex tube (Fig. 1) is a device that expands a flow and separates it into two streams with one having a lower enthalpy (or temperature) than the inlet's and another having a higher enthalpy (or temperature). This phenomenon is known as energy (temperature) separation. The integration of vortex tube in experimental prototypes of heat pump is still lagging behind. Moreover, studies discussing vortex tube heat pumps considered the vortex tube as a black box without taking into account the complex separation process at play. Dubey *et al.* (2015) constructed an analytical model to resemble a cascade heat pump system using propylene as refrigerant for the lower cycle and CO_2 for the upper vortex tube cycle. The upper cycle is based on Maurer's model (Maurer & Zinn, 1999) which assumes that the liquid formed after the vortex tube nozzle is separated completely from the vapor or gas streams. Using their analysis, the maximum improvement in terms of COP_h is 5.9% compared to a transcritical cascade cycle without a vortex tube. Patil *et al.* (2020) analyzed thermodynamically the energetic and exergetic efficiencies of several different transcritical CO_2 heat pump systems including a vortex tube heat pump (VTHP) based on the Maurer's model. They concluded that the VTHP showed moderate improvement in COP_h by 3% over the CHP. For the second law efficiency, the performance of the VTHP was moderate, even though the exergy lost in vortex tube was relatively the highest among other studied expansion devices.

In this paper, a transcritical CO_2 heat pump system integrating a vortex tube is analyzed and compared to a conventional heat pump. The novelty of this work lies within the implementation of a two-phase fluid thermodynamic model of the vortex tube that was developed by Mansour *et al.* (2022a, 2022b). Furthermore, the objective is to prove that integrating a vortex tube into a simple heat pump configuration can provide more benefits over a corresponding conventional cycle. The software Dymola is used as the simulation tool while the TIL library is relied on to access thermodynamic models of other heat pump components. The article is presented as follows: the methodology is presented in Section 2, the validation of the TIL library model is presented in Section 3 and the results are discussed in Section 4.

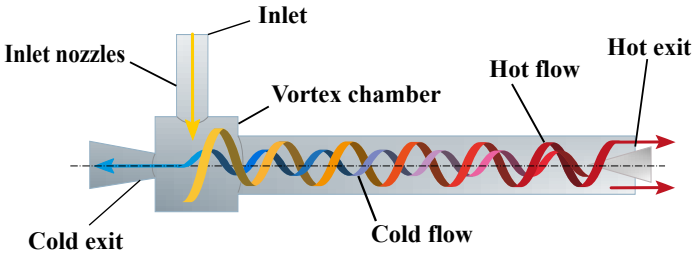

Figure 1: A schematic representation of a counter-flow vortex tube.

2. METHODOLOGY

The thermodynamic model of the heat pump used in this study is built using the models provided by the commercial TIL library. It provides different models for many components including compressors, heat exchangers and valves. Only the vortex tube model is not provided by this library, and the model developed and validated by Mansour *et al.* (2022a, 2022b) is used.

2.1 Vortex tube heat pump cycle

The schematic VTHP cycle simulated in this work is shown in Fig. 2 while a corresponding pressure-enthalpy diagram of the cycle is presented in Fig. 3. Superheated CO_2 is compressed to supercritical condition (1) by the compressor. The fluid is then cooled through a gas cooler after which it enters the vortex tube (2). The flow then expands in the vortex tube nozzles (2*) and, afterwards, splits into low (3) and high (4) enthalpy (temperature) flows inside the vortex tube. These flows will be referred to as cold exit (3) and hot exit (4) flows, respectively. The hot exit flow is then passed through a desuperheater (5) to release heat. Afterwards, this flow is expanded (6) and then mixed with the cold exit flow exiting from the other side of the vortex tube (7). The combined flow passes through the evaporator and then into a separator (8) to remove any remaining liquid CO_2. Finally the flow moves back to the compressor (9).

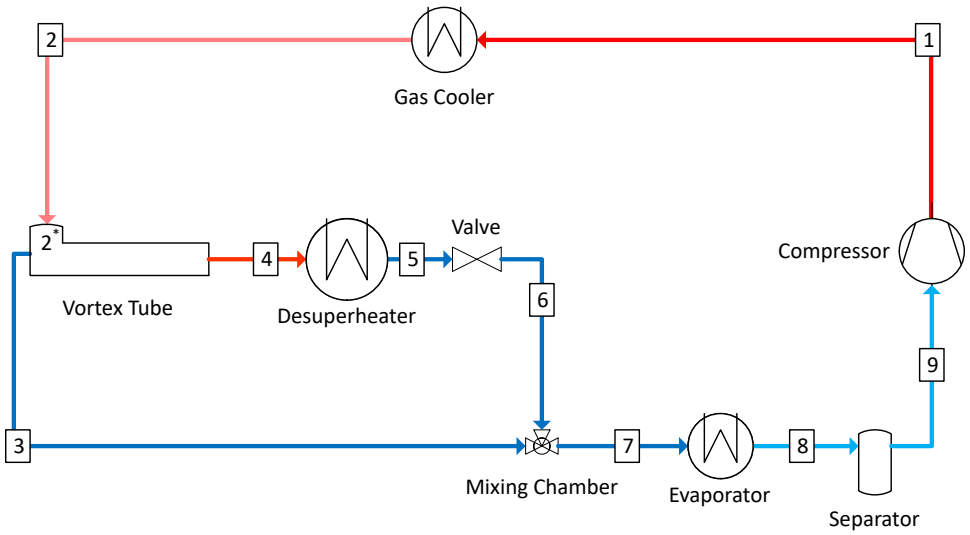

Figure 2: Schematic representation of the transcritical CO_2 VTHP cycle.

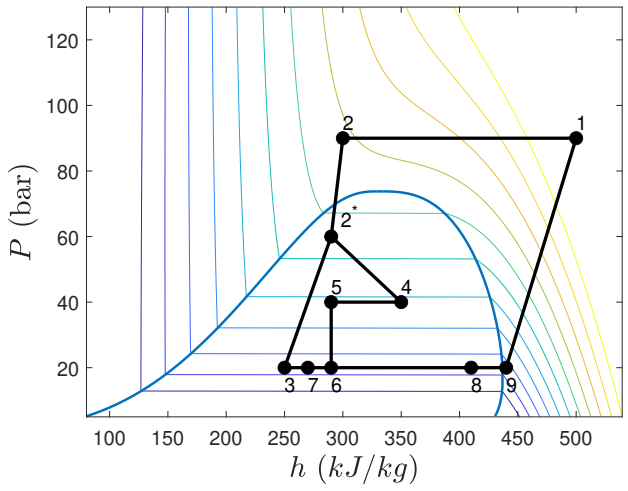

Figure 3: Pressure-enthalpy diagram of the transcritical CO_2 VTHP cycle shown in Fig. 2.

2.2 Compressor

The TIL library provides different compressor models varying from simple to sophisticated ones. The more precise, sophisticated models are type-specific and can provide more accurate results. However, they require more input data that might not be available, hence, making their implementation harder. The model used in the present study is an efficiency based model that depends on the compressor speed, displacement and three efficiency parameters, namely

volumetric, isentropic and overall isentropic efficiencies. The three definitions of the efficiencies are used to calculate three different quantities of the cycle. To calculate the mass flow rate ($\dot{m}_{CO_2}$), the volumetric efficiency equation is used:

$$\eta_{vol} = \frac{\dot{m}_{CO_2}}{V_{disp} n \rho_{suc}} \tag{1}$$

where η_{vol}, V_{disp}, n and ρ_{suc} are volumetric efficiency, volumetric displacement, compressor speed and suction density, respectively.

To calculate the actual discharge enthalpy (h_{dis}), the isentropic efficiency is used to account for the deviation from the ideal compression process:

$$\eta_{is} = \frac{h_{dis,is} - h_{suc}}{h_{dis} - h_{suc}} \tag{2}$$

where η_{is}, $h_{dis,is}$ and h_{suc} are isentropic efficiency, isentropic discharge enthalpy and suction enthalpy, respectively.

Finally, to compute the compressor power (W_{comp}), the overall isentropic efficiency ($\eta_{is,o}$) equation is utilized:

$$\eta_{is,o} = \frac{\dot{m}(h_{dis,is} - h_{suc})}{W_{comp}} \tag{3}$$

2.3 Heat Exchangers

The TIL library also offers a variety of heat exchanger models. The chosen model is selected based on the geometry of the heat exchanger. In addition, each model offers variant methods to calculate the heat transfer coefficients. It is based on the finite volume approach, which segments each flow path in the heat exchanger into cells. The selected heat exchanger geometry in this study for either the gas cooler, evaporator or desuperheater is the counter-flow plate heat exchanger. It requires the knowledge of several geometrical parameters that can be supplied by the manufacturer including the number of plates, length, width and inclination angle.

In order to calculate the heat transfer coefficient on the refrigerant side for a single-phase superheated fluid (α_{sh}), the following equation is implemented:

$$\alpha_{sh} = 0.277 \left(\frac{\lambda}{d_H} \right) Re^{0.766} Pr^{1/3} \tag{4}$$

where Re, Pr, λ and d_H are Reynolds number, Prandtl number, fluid thermal conductivity and hydraulic diameter, respectively.

Meanwhile, the heat transfer coefficient for single-phase subcooled refrigerant (α_{sc}) is calculated as follows:

$$\alpha_{sc} = 0.2267 \left(\frac{\lambda}{d_H} \right) Re^{0.631} Pr^{1/3} \tag{5}$$

On the other hand, for the two-phase refrigerant fluid, special correlations were developed for evaporation by Longo, Mancin, *et al.* (2015). The correlations were developed for brazed plate heat exchangers. Firstly, they calculated the heat transfer coefficient using two boiling mechanisms: convective and nucleate. The heat transfer coefficient based on the convective boiling (α_{cb}) is computed as follows:

$$\alpha_{cb} = 0.122 \varphi \left(\frac{\lambda}{d_H} \right) Re_e^{0.8} Pr^{1/3} \tag{6}$$

where φ and Re_e are the enlargement factor of the plates and equivalent Reynolds number calculated using the mean vapor quality between the inlet and output, respectively.

The calculation of the heat transfer coefficient based on the nucleate boiling (α_{nb}) writes:

$$\alpha_{nb} = 0.58\varphi\alpha_0 C_{Ra} F(P^*) \left(\frac{q}{20000}\right)^{0.467} \tag{7}$$

where α_0 is a reference heat transfer coefficient determined based on the refrigerant, $C_{Ra} = \left(\frac{R_a}{0.4}\right)^{0.1333}$ is a coefficient which accounts for the effect of arithmetic mean roughness R_a of the plates, $\left(\frac{q}{20000}\right)^{0.467}$ is a term accounting for the heat flux and $F(P^*) = 1.2P^{*0.27} + \left(2.5 + \frac{1}{1-P^*}\right)P^*$ is a term that accounts for the effect of reduced pressure p^*.

Secondly, they selected the two-phase refrigerant heat transfer coefficient as the maximum coefficient resulting from the two mechanisms. However, the multiplication of the boiling number (*Bo*) and Martinelli parameter (*Xtt*) is the criterion used instead to determine the two-phase flow heat transfer coefficient by the library. The criterion is:

- If $(Bo \times Xtt < 0.00015)$ then the convective boiling mechanism is selected.
- If $(Bo \times Xtt > 0.00015)$ then the nucleate boiling mechanism is selected.

For a two-phase refrigerant that is going through a condensation process, Longo, Righetti, and Zilio (2015) presented two condensation mechanisms (gravity-dominated condensation and forced convection condensation) for brazed plate heat exchanges that are distinguished by the value of the equivalent Reynolds number, Re_e:

- If $(Re_e < 1600)$ then the gravity-dominated condensation is selected.
- If $(Re_e > 1600)$ then the forced convection condensation is selected.

The heat transfer coefficient based on gravity-dominated condensation is calculated as:

$$\alpha_{gd} = 0.943\varphi \left(\frac{\lambda^3 \rho_L^2 g \Delta J_{LG}}{\mu \Delta T L}\right)^{1/4} \tag{8}$$

where ρ_L is the condensate density, g is the gravitational acceleration, ΔJ_{LG} is the condensation latent heat, μ is the dynamic viscosity, ΔT is the difference between saturation and wall temperatures and L is the plate length.

Meanwhile, the heat transfer coefficient based on the forced convection condensation is as follows:

$$\alpha_{fc} = 1.875\varphi \left(\frac{\lambda}{d_H}\right) Re_e^{0.445} Pr^{1/3} \tag{9}$$

To calculate the heat transfer coefficient of the external fluid of either the gas cooler, the desuperheater or the evaporator, the correlation presented by Martin (1996) is used:

$$\alpha_{ef} = 0.122 Pr^{1/3} \left(\frac{\eta}{\eta_{wall}}\right)^{1/6} \left(\frac{\lambda}{d_H}\right) \left(\zeta Re^2 sin(2\varphi)\right)^{0.374} \tag{10}$$

where $\left(\frac{\eta}{\eta_{wall}}\right)^{1/6}$ is a correction factor accounting for the liquid viscosity and ζ is a friction factor.

2.4 Vortex Tube

The thermodynamic model introduced by Mansour *et al.* (2022a, 2022b) is implemented in this work to represent the vortex tube. The model objective is to mainly compute the enthalpies and temperatures of cold and hot exits. It is mainly dependent upon 3 processes. The first one is the isentropic expansion in the inlet nozzles. The second process is the calculation of the pressure gradient in the vortex chamber, which is represented by a simplified radial momentum equation:

$$\frac{\partial P(r)}{\rho(r)} = \frac{u_\theta^2 \partial r}{r} \tag{11}$$

where $P(r)$ is the radial pressure distribution, $\rho(r)$ is the radial density distribution, u_θ is the tangential velocity and r is the local radius.

The final is the conservation of energy which is specifically used to calculate properties downstream of the vortex tube based on the properties computed upstream:

$$h_{0h} = \frac{h_{0in} - \mu_c h_{0c}}{(1 - \mu_c)} \tag{12}$$

where h_{0in}, h_{0h}, h_{0c} and μ_c are the inlet total enthalpy (gas cooler exit enthalpy), the hot exit total enthalpy (desuperheater inlet enthalpy), the cold exit total enthalpy and the cold mass fraction which is the ratio of the cold exit mass flow rate to the inlet mass flow rate, respectively.

2.5 Performance Analysis

In order to estimate the heat pump performance, two conventional performance parameters are implemented. The first is the heating capacity of both the gas cooler ($Q_{h,gc}$) and the desuperheater ($Q_{h,des}$) defined as:

$$Q_{h,gc} = \dot{m}_{CO_2} \left(h_{gc,in} - h_{gc,out} \right) \tag{13}$$

where $h_{gc,in}$ and $h_{gc,out}$ are the enthalpies of the inlet and exit, respectively, of the gas cooler.

$$Q_{h,des} = (1 - \mu_c) \dot{m}_{CO_2} \left(h_{des,in} - h_{des,out} \right) \tag{14}$$

where $h_{des,in}$ and $h_{des,out}$ are the enthalpies of the inlet and exit, respectively, of the desuperheater.

The second performance parameter is the overall coefficient of performance (COP_h):

$$COP_h = \frac{Q_{h,gc} + Q_{h,des}}{W_{comp}} \tag{15}$$

3. VALIDATION

Based on the authors' knowledge, no experimental data could be found on heat pumps integrating vortex tubes to directly validate a full vortex tube heat pump model. Therefore, the study is reliant on the validation of the vortex tube model that was previously conducted by Mansour *et al.* (2022a, 2022b) in addition to the validation of the models of the TIL library using experimental data provided by the Laboratoire des Technologies de l'Énergie of Hydro-Québec, which is presented in this article. The provided experimental data are from an ejector cascade cycle, part of which is a conventional CO_2 sub-cycle while the other part is an R245fa ejector sub-cycle. The validation is only conducted on the CO_2 sub-cycle for the purpose of simplicity and for the lack of an ejector model validated with R245fa.

The compressor model used is a Bitzer transcritical CO_2 (4MTE-10K) operated in subcritical mode at a speed of 1750 RPM and a displacement of 76.34 cm^3. The evaporator model is similar to the commercial model Kaori C200, meanwhile, the intercooler model is similar to the model Kaori C201. The main refrigerant of the cycle is CO_2, the heat source fluid of the evaporator is 50/50 ethylene glycol/water mixture and the refrigerant passing through the opposite side of the intercooler is R245fa. Based on the operational experimental data provided, Table 1 shows the independent inputs of the system.

Table 2 concludes the results of the validation process of a heat pump model created using the TIL library. The model shows a fairly good agreement in comparison with the experimental data. The error of every parameter is within an acceptable range except for the heating capacity in the intercooler from CO_2 to R245fa where the error reaches 15%. This might be due to the heat transfer coefficient model which can produce increased error in the prediction of the coefficient as it was shown in the study of Longo, Mancin, *et al.* (2015). However, the same model seems to produce very good prediction of the cooling capacity with CO_2.

Table 1: Input data of the validation simulation of subcritical CO_2 CHP.

Input Parameter	Value
P_{R245fa} (bar)	1.06 (saturated vapor)
$\dot{m}_{R245fa}$ (kg/s)	0.138
$\dot{m}_{glycol}$ (kg/s)	0.976
T_{glycol} (K)	267.11
η_{vol}	0.81
η_{is}	0.64
$\eta_{is,o}$	0.62

Table 2: Comparison of experimental results against the TIL model.

Parameter	Experiment	Model	Error %
P_{dis} (bar)	53.3	53.95	1.2
P_{suc} (bar)	21.69	21.29	1.85
T_{dis} (K)	352.1	354.8	0.8
T_{suc} (K)	267.5	267.1	0.1
$\dot{m}_{CO_2}$ (kg/s)	0.093	0.095	2.8
W_{comp} (kW)	6.125	6.552	7
Q_h (kW)	26.957	22.808	15.4
Q_c (kW)	17.072	16.485	3.4

4. RESULTS AND DISCUSSION

In this part, a parametric analysis of different parameters is conducted to test their effects on the VTHP and exhibit how it can improve the efficiency over the conventional heat pump. Regarding the evaporator, the same conditions and characteristics used in the validation are still implemented in the parametric analysis. In addition, the compressor specifications are also kept the same. For the gas cooler and the desuperheater, the same geometrical characteristics of the validation intercooler are implemented. Taslimi Taleghani *et al.* (2019) used a 50/50 ethylene glycol/water mixture as a heat sink for the gas cooler. Hence, for the current study, the same fluid will be used for both the gas cooler and the desuperheater. Meanwhile, for the operational inputs of the gas cooler, the mass flow rate of ethylene glycol/water mixture is 0.656 kg/s while the inlet temperature is 320 K. For the desuperheater, the ethylene glycol/water mixture mass flow rate is 0.656 kg/s and the inlet temperature is 276 K. The desuperheater CO_2 pressure (P_{des}) is 40 bar. The cold mass fraction of the vortex tube is kept constant at 0.5, even though its variation will not have a noticeable effect on performance as it will be discussed later on. Finally, the geometrical dimensions of the vortex tube used in this study are the same as those used by Mansour *et al.* (2022a, 2022b). It is worth mentioning that the operational limits of the compressor were respected, hence, restricting the assessed range of the parameters.

The first controlling parameter that is tested in this article is the discharge pressure. Varying P_{dis} does not directly reflect the varying effect of integrating a vortex tube. However, it gives an idea about how the presence of a vortex tube (and an extra heat exchanger) can add up to the cycle performance. Fig. 4a exhibits the variation of the overall heating capacities of both VTHP and CHP. In addition, the figure shows the capacities of the gas cooler and the desuperheater components of the VTHP cycle. The gas coolers of both cycles exhibit very similar results. Yet, the overall heating capacity of VTHP is significantly higher by a maximum of 30.9% over the whole examined discharge pressures taking into account the heating capacity of the desuperheater. An interesting observation is that the desuperheater heating capacity is invariant with the pressure which is attributed to two reasons. The first one is because the hot exit flow, under the current operating conditions, is a two-phase flow for almost all tested values of P_{dis}. And since P_{des} is kept constant at 40 bar, the temperature also stays constant, even though the enthalpy changes. The second is that the ethylene glycol/water mixture input temperature of 276 K is close to the hot exit flow saturation temperature. Thus, this facilitates reaching the maximum heating capacity that can be supplied by the heat exchanger at the stated conditions.

Fig. 4b presents the COP_h of both VTHP and CHP cycles. As a direct effect of the superior heating capacity of the VTHP over the CHP, the VTHP shows a remarkable advantage compared to the CHP. The maximum increase in COP_h

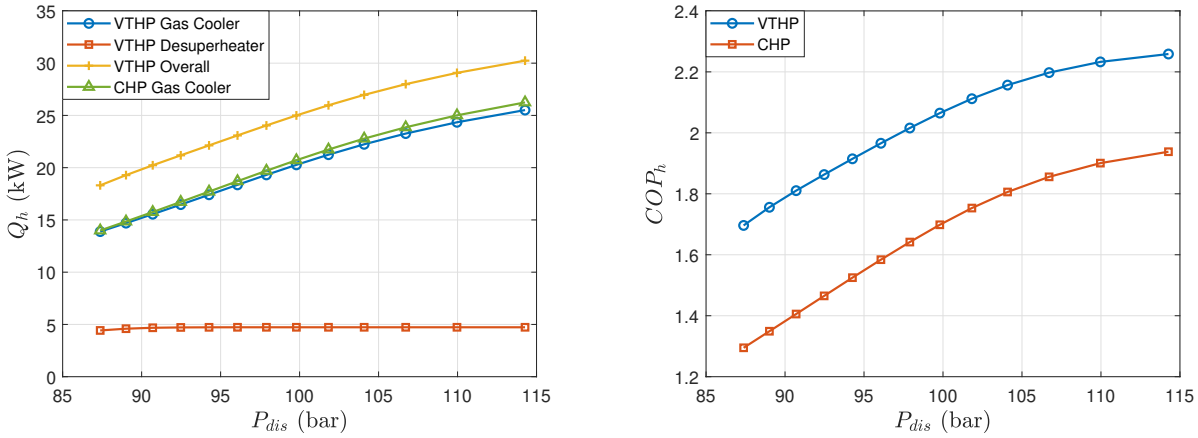

Figure 4: (a) Heating capacity change with the discharge pressure for both VTHP and CHP. (b) Corresponding variation of overall COP_h of each cycle with the discharge pressure.

of the VTHP cycle from the CHP cycle reaches 31 % at the lowest pressure of 87 bar. This increase in COP_h between both systems decreases as P_{dis} rises. However, it stays still significant with the COP_h increasing by 16.5 % at the highest pressure of 114 bar. It can also be noticed that the rate of COP_h increase for each cycle with P_{dis} is higher at lower pressures. This might indicate that the performance can reach an optimum COP_h value at a higher P_{dis}. However, it was not possible to fully investigate this due to the limitations imposed by the compressor on the operating pressures as well as the operating inputs implemented in this study.

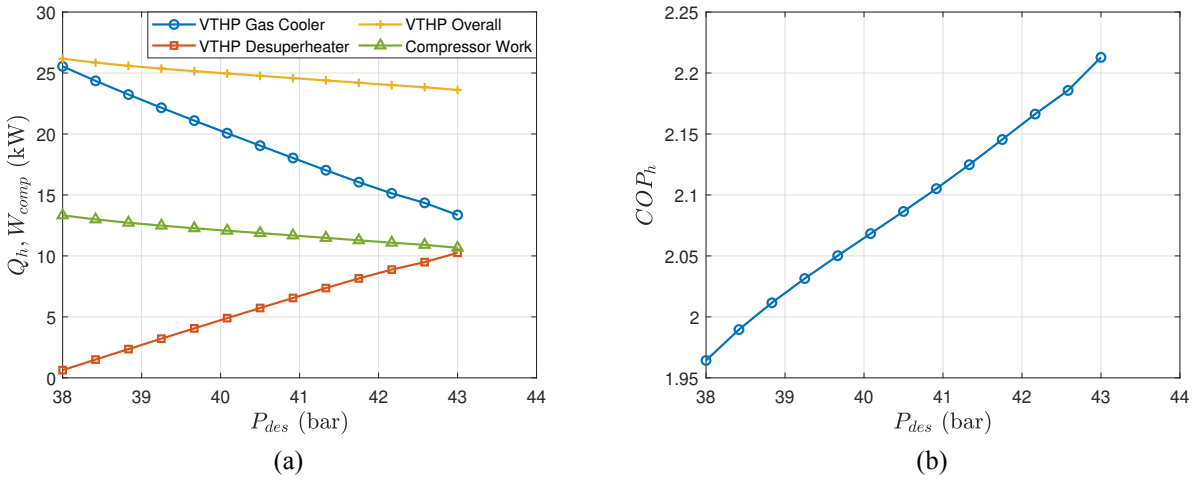

Figure 5: (a) Heating capacity change with the desuperheater pressure of the VTHP cycle. (b) Variation of the overall COP_h of the VTHP cycle with the desuperheater pressure.

The second varying parameter considered to increase the VTHP performance is the desuperheater pressure. Using the simulation model, P_{des} is adjusted using a PI controller that varies the area of the valve using a feedback loop with a defined input by the user. Lowering or raising P_{des} has a direct effect on the amount of heat extracted from the hot exit flow of the vortex tube, since consequently, the CO_2 flow temperature also varies with P_{des}. Fig. 5a shows a detailed presentation of the effect of the desuperheater pressure, at a constant $\dot{m}_{CO_2}$ of 0.126 kg/s, on the heating capacity of the gas cooler, the desuperheater and the combination of both of them in addition to the compressor power of the cycle. The desuperheater capacity increases with P_{des} as a direct effect of the simultaneous rise in temperature of the vortex

tube hot exit flow. On the other hand, both the gas cooler capacity and compressor work decrease. Combining the effect of both the gas cooler and desuperheater, the resulting overall capacity of the cycle presents a decreasing manner with P_{des}. Meanwhile, as P_{des} increases, the overall COP_h of the cycle also increases (Fig. 5b). Hence, if the sole performance criterion is the heating capacity, integrating a vortex tube along with a desuperheater might not be the best idea under the studied conditions. Yet, putting the compressor work into consideration makes a huge difference in the decision as it is noticed in Fig. 5b of the COP_h. In addition, within the considered range of P_{des}, the overall heating capacity decreases by 9.8 % while the compressor work decreases by 20 %, which mainly explains the significantly increasing COP_h. A P_{des} value of 38 bar is selected as the lowest tested value due to the restricting limitations of the compressor. In addition, a lower value than 38 bar would induce that the desuperheater would act as an evaporator, hence, lowering the overall heating capacity of the system. On the other hand, the maximum tested value is limited at 43 bar because afterwards the system operating regime transforms from transcritical into subcritical, which is out of the scope of the current work.

Finally, the effect of the cold mass fraction was studied. However, it did not provide any improvement to the system. Varying it changes mainly the enthalpies of the exiting flows of the vortex tube. Yet, for the hot exit, this is not enough to raise the temperature of the flow and, thus, increase the desuperheater capacity as the hot exit flow is mostly in two-phase condition.

It should be mentioned that operating the vortex tube under certain transcritical conditions can limit the parameters used to control the benefits of implementing a vortex tube with a desuperheater, which is reflected on the variation of the discharge pressure as well as the cold mass fraction. However, the advantage of incorporating a vortex tube is definitely guaranteed based on what was obtained with simulations conducted within the frame of this work. Different operating conditions might deem to be necessary to uncover the full potential of implementing a VTHP system.

5. CONCLUSIONS

In this article, a vortex tube heat pump system operating with transcritical CO_2 was investigated using thermodynamic modeling on Dymola. The thermodynamic models of the heat pump components were validated within the frame of this study except the vortex tube model, which was validated in previous studies. The validation results were deemed very acceptable to perform a study on the effect of integrating a vortex tube. Afterwards, it was shown that a VTHP cycle can provide a significant performance improvement over the CHP system. The maximum increase in the overall Q_h between both cycles is 30.9 % while the maximum increase in COP_h is 31 %. In addition, the effects of the desuperheater pressure as well as the cold mass fraction of the vortex tube were discussed. It was found that a compromise should be reached to find the optimum desuperheater pressure that can provide the most suitable heating capacity with lower compressor work based on the application and operating conditions. Finally, under the tested operating inputs, the cold mass fraction has no effect on the VTHP heating performance due to the presence of the two-phase condition of the hot exit flow.

As future projections, this work is to be extended to extensively study more parameters and on a wider range. Moreover, experiments are to be performed to study the feasibility and practicality of investing in such system.

NOMENCLATURE

Acronyms

CHP	conventional heat pump
CO_2	carbon dioxide
COP_h	heating coefficient of performance
VTHP	vortex tube heat pump

Indices

0	total (stagnation), reference
θ	tangential
c	cold exit, cooling
cb	convective boiling
des	desuperheater
dis	discharge
disp	displacement
e	equivalent
ef	external fluid
fc	forced convection
gc	gas cooler
gd	gravity-dominated
H	hydraulic
h	hot exit, heating
is	isentropic
L	condensate
nb	nucleate boiling
o	overall
sc	subcooled
sh	superheated
suc	suction
vol	volumetric

Symbols

α	heat transfer coefficient	(W m^{-2} K)

$\dot{m}$	mass flow rate	(kg s^{-1})	n	compressor speed	(rpm)
η	efficiency	(-)	p	pressure	(Pa)
λ	thermal conductivity	(W m^{-1} K^{-1})	Pr	Prandtl number	(-)
μ	mass fraction	(-)	Q	capacity	(W)
φ	enlargement factor	(-)	q	heat flux	(W m^{-2})
ρ	density	(kg m^{-3})	r	radius	(m)
ζ	friction factor	(-)	R_a	surface roughness	(m)
Bo	boiling number	(-)	Re	Reynolds number	(-)
d	diameter	(m)	u	tangential velocity	(m s^{-1})
F	reduced pressure factor	(-)	V	volume	(m^3)
g	gravitational acceleration	(m $s^{-}2$)	W	work	(W)
h	specific enthalpy	(J kg^{-1})	X_{tt}	Martinelli parameter	(-)
L	heat exchanger plate length	(m)			

REFERENCES

Chen, W. (2008). A comparative study on the performance and environmental characteristics of R410A and R22 residential air conditioners. *Applied Thermal Engineering*, *28*(1), 1-7.

Chua, K., Chou, S., & Yang, W. (2010). Advances in heat pump systems: A review. *Applied Energy*, *87*(12), 3611-3624.

Dubey, A., Agrawal, G., & Kumar, S. (2015). Performance evaluation and optimal configuration analysis of a transcritical carbon dioxide/propylene cascade system with vortex tube expander in high-temperature cycle. *Clean Technologies and Environmental Policy*, *18*, 1-18.

Hakkaki-Fard, A., Aidoun, Z., & Ouzzane, M. (2015). Improving cold climate air-source heat pump performance with refrigerant mixtures. *Applied Thermal Engineering*, *78*, 695-703.

Junqi, D., Yibiao, W., Shiwei, J., Xianhui, Z., & Linjie, H. (2021). Experimental study of R744 heat pump system for electric vehicle application. *Applied Thermal Engineering*, *183*, 116191.

Longo, G. A., Mancin, S., Righetti, G., & Zilio, C. (2015). A new model for refrigerant boiling inside brazed plate heat exchangers (BPHEs). *International Journal of Heat and Mass Transfer*, *91*, 144-149.

Longo, G. A., Righetti, G., & Zilio, C. (2015). A new computational procedure for refrigerant condensation inside herringbone-type brazed plate heat exchangers. *International Journal of Heat and Mass Transfer*, *82*, 530-536.

Mansour, A., Lagrandeur, J., & Poncet, S. (2022a). Analysis of transcritical CO_2 vortex tube performance using a real gas thermodynamic model. *International Journal of Thermal Sciences*, *177*, 107555.

Mansour, A., Lagrandeur, J., & Poncet, S. (2022b). Vortex tube thermodynamic model operating with two-phase fluids. In *Heat powered cycles 2021 conference proceedings.* Bilbao, Spain.

Martin, H. (1996). A theoretical approach to predict the performance of chevron-type plate heat exchangers. *Chemical Engineering and Processing: Process Intensification*, *35*(4), 301-310.

Maurer, T., & Zinn, T. (1999). Untersuchung von Entspannungsmaschinen mit mechanischer Leistungsauskopplung für die transkritische CO_2-Kältemaschine. *DKV-Tagungsbericht*, *26*, 264 – 277.

Patil, O. S., Shet, S. A., Jadhao, M., & Agrawal, N. (2020). Energetic and exergetic studies of modified CO_2 transcritical refrigeration cycles. *International Journal of Low-Carbon Technologies*, *16*(1), 171-180.

Taslimi Taleghani, S., Sorin, M., Poncet, S., & Nesreddine, H. (2019). Performance investigation of a two-phase transcritical CO_2 ejector heat pump system. *Energy Conversion and Management*, *185*, 442-454.

Wang, D., Yu, B., Hu, J., Chen, L., Shi, J., & Chen, J. (2018). Heating performance characteristics of CO_2 heat pump system for electrical vehicle in a cold climate. *International Journal of Refrigeration*, *85*, 27-41.

ACKNOWLEDGMENT

The authors acknowledge the NSERC chair on industrial energy efficiency established in 2019 at Université de Sherbrooke with the support of Hydro-Québec, Natural Resources Canada and Emerson Commercial and Residential Solutions.